Enhanced Coil Expansion and Intrapolymer Complex Formation of Linear Poly(methacrylic acid) Containing Poly(ethylene glycol) Grafts†

Garrett D. Poe, William L. Jarrett, Charles W. Scales, and Charles L. McCormick*

Department of Polymer Science, University of Southern Mississippi, Southern Station Box 10076, Hattiesburg, Mississippi 39406-0076

Received August 25, 2003; Revised Manuscript Received January 6, 2004

ABSTRACT: Poly(methacrylic acid) (PMA) and poly(ethylene glycol) (PEG) represent a polyacid/polybase pair capable of forming reversible, pH-responsive, hydrophobic complexes stabilized by hydrogen bonding in aqueous media. Linear PMA was modified with methoxy-terminated, long-chain (5000 M_w) poly(ethylene glycol) (MPEG) via random coupling in dimethyl sulfoxide using dicyclohexylcarbodiimide as a coupling agent. The degree of ionization, α, was deteremined utilizing potentiometric titration. The presence of tethered MPEG markedly increased the pK_a values over those of the PMA homopolymer or PMA/MPEG mixtures at $\alpha < 0.35$. The dilute solution PMA−PEG intramolecular association was probed by monitoring the PEG nuclear magnetic resonance (NMR) spin−spin (T_2) relaxation as a function of pH. Two populations of MPEG exist at appropriate ionizations: those participating in hydrogen bonding with the PMA backbone and those not participating in hydrogen bonding. Polymer self-diffusion at varying degrees of ionization was measured using pulsed gradient spin echo (PGSE) NMR and dynamic light scattering. Acidic conditions produced coil collapse, apparently arising from the formation of intramolecular hydrogen-bonded complexes along the polymer backbone. Under basic conditions, coil expansion was observed due to conformational changes (polyelectrolyte effect), and the added volume of the tethered MPEG as well as the reduction of intramolecular complexation as the number of carboxylate anions increased.

Introduction

The manipulation of polymer hydrodynamic volume in response to external stimulus is useful in drug delivery, enhanced oil recovery, drag reduction, and water remediation.[1−5] Polymers effective in these applications are designed to respond to a particular environmental stimulus, most commonly temperature, electrolytes, or solution pH.[2−7] Typically, these systems consist of associating moieties covalently attached to a flexible water-soluble polymer backbone and associate by means of dipole−dipole, ion−ion, hydrogen-bonding, or hydrophobic interactions. The associative mechanisms are not limited to the localized interactions between two interacting components but also extend to polymer−polymer complexation.

Interpolymer complexes have been observed for oppositely charged polyions (interpolyelectrolyte complex), oppositely handed polymers, and hydrogen-bonding polyacid/polybase pairs.[8−17] Hydrogen-bonding polymer pairs have been investigated utilizing viscometry, fluorescence, potentiometric and conductiometric titrations, and NMR spectroscopy.[10,11,14,15,18,19] The complex-forming ability depends on the chemical compositions and stoichiometry of the participating repeat units, the molecular weights of the contributing polymer chains, and the environmental solvent conditions.[11] The solution pH, temperature, and electrolyte concentration affect complexation and prove useful as stimuli for formation and dissociation of hydrogen-bonding polymer pairs.[11,20]

A large portion of research in hydrogen-bonding polymer pairs has concentrated on the hydrogen-bonding complex between poly(carboxylic acid)s such as poly(acrylic acid) (PAA) or poly(methacrylic acid) (PMA) and poly(ethylene glycol) (PEG) in aqueous media.[10,14,18,19,21−25] Certain features have been quantitatively verified through experiment: hydrogen-bonding polymer pairs generally form a stoichiometric 1:1 acid/base repeat unit ratio; complex stability increases with the molecular weights of each component; resultant complexes are more hydrophobic than either of the contributing chains.[12,25,26]

The swelling behavior of poly(methacrylic acid)-*g*-poly(ethylene glycol) hydrogel networks in response to pH, temperature, copolymer composition, and cross-link density has been examined by swelling uptake, fluorescence, and solute diffusion studies.[27−29] Complex formation in grafted copolymers was shown to occur over a wider range of molecular weights as compared to their homopolymer analogues, presumably due to a restriction in chain mobility.

The solution synthesis of a series of nongelling poly(methacrylic acid)-*g*-poly(ethylene glycol) copolymers has been previously reported, and using computer modeling and oil-uptake experiments, a model was proposed in which the hydrophilic main chain of PMA contains short patches of hydrophobic complexes capable of subsequent hydrophobic association.[12,13]

However, despite the versatility of the synthetic approach (free-radical polymerization in 80:20 ethanol:water) employed to obtain these polymers, there are also inherent limitations. The average molecular weight of copolymers synthesized has been shown to vary inversely with the PEG in the feed over orders of magnitude due to chain transfer to PEG.[30] The comparison of linear poly(methacrylic acid)-*g*-poly(ethylene glycol) with varying degrees of PEG incorporation is necessarily qualitative because of the molecular weight differences, and the length of the PMA backbone decreases with increasing PEG feed. In addition, the presence of ethanol as a polymerization solvent limits the molecular weight of the formed polymers, making it difficult to

† Paper number 103 in a series titled Water Soluble Polymers.
* To whom correspondence should be addressed.

10.1021/ma035261i CCC: $27.50
Published on Web 03/02/2004

obtain moderate molecular weight polymers necessary for some applications. Third, PEG chains with methacrylate headgroups form micelles in water and water/solvent mixtures, leading to microblocky incorporation.[31]

The work described in this paper utilizes grafting reactions in organic media in an attempt to minimize the above issues: the number of backbone residues can be kept constant for any degree of PEG incorporation; the final molecular weight is controlled by the original molecular weight of the PMA and the incorporation of PEG side chains; and the PEG is likely to be incorporated at random, rather than blocky. This article describes the synthesis of such PMA-*g*-PEG copolymers and examines the PEG side-chain contribution to coil expansion and collapse. The pH-responsive intrapolymer (dilute solution) complex formation is probed using potentiometric titrations and local-level spin−spin (T_2) NMR relaxation measurements. The long-range diffusion properties are examined with pulsed-gradient spin echo (PGSE) NMR and dynamic light scattering.

Experimental Section

Materials. Poly(ethylene glycol) monomethyl ether M_w 5000 (MPEG, 99%, degree of polymerization ≈ 114) was obtained from Aldrich with dihydroxy content reported less than 1 mol % and used without further purification. Methacrylic acid (MAA) was vacuum-distilled at 40 °C immediately prior to use. 2,2′-Azobis(isobutyronitrile) (AIBN) was obtained from Aldrich and recrystallized from ethanol prior to use. (*N*,*N*-Dimethylamino)pyridine (DMAP, 99%), dicyclohexylcarbodiimide (DCC, 99%), and dimethyl sufloxide (DMSO, 99.9+%) were obtained from Aldrich and used without further purification. Benzene (99+% spectrophotometric grade) was obtained from Burdick and Jackson and used without further purification. Deionized water was obtained from a Milli-Q Millipore system, with a resistivity of 17.8 Ω·cm. Gas chromatography or ^{1}H NMR was used to determine the purity of all compounds.

Synthesis of Poly(methacrylic acid) (PMA). Poly(methacrylic acid) was synthesized via polymerization in benzene. Freshly distilled MAA (21.53 g, 0.250 mol) was heated in 250 mL of benzene to 60 °C under gentle stirring and dry nitrogen sparge and initiated with 0.215 g of AIBN. The polymerization was terminated with acetone after 1 h, and the precipitate was purified with benzene in a Soxhlet apparatus. The recovered white polymer was dried in vacuo at 45 °C for 48 h to yield 8.42 g (39.1%). ^{1}H NMR (D_2O): δ = 1.84 methacrylate CH_2; δ = 0.92 methacrylate CH_3. ^{13}C NMR (d_6-DMSO): δ = 188.5−179.2, C═O; δ = 54.1−51.5, quaternary carbon; δ = 45.1−44.7, CH_2; δ = 20.6−16.9, CH_3. The molecular weight was determined by static light scattering and Zimm plot analysis in 0.5 M NaCl, pH 9.5, to be 5.8×10^5 g/mol.

Synthesis of Poly(methacrylic acid)-*g*-poly(ethylene glycol) (PMA-*g*-MPEG). A series of poly(methacrylic acid)-*graft*-poly(ethylene glycol) (PMA-*g*-MPEG) copolymers incorporating methoxy-terminated poly(ethylene glycol) (MPEG) in different amounts were synthesized by adjusting the MPEG (M_w 5000 g/mol) feed with a constant quantity of poly(methacrylic acid) (M_w 580 000 g/mol), using a reaction procedure modified from a scheme previously reported in the literature.[30] The number of MPEG grafted chains was therefore varied while maintaining a constant PMA backbone length. In a typical procedure, a reaction vessel was charged with PMA (1.50 g, 0.0174 mol) dissolved in 100 mL of DMSO and sparged with dry nitrogen for 2 h at room temperature under gentle stirring. DCC (3.95 g, 0.0192 mol), DMAP (0.232 g, 0.00192 mol), and MPEG (2.30 g, 0.0522 mol) were dissolved separately in 50 mL of DMSO, then injected into the reaction vessel, and stirred for 48 h at room temperature under nitrogen. White dicyclohexylurea, a side product of the DCC coupling reaction, formed during the reaction and was removed by filtration. Poly(methacrylic acid)-*g*-poly(ethylene glycol) was precipitated by the addition of 12 mL of 8.75 M NaOH, isolated by filtration, and washed with hot DMSO and room temperature ethanol. Recovered polymer was dissolved in 800 mL of deionized water, filtered to remove residual insoluble dicyclohexylurea, and purified in an ultrafiltration apparatus, molecular weight cutoff 30 000, until permeate reached pH 7. Bright white polymer (1.13 g, 29.7%) was recovered by lyophilization. ^{1}H NMR (D_2O): δ = 4.01, ester CH_2; δ = 3.65, MPEG CH_2; δ = 3.32, MPEG CH_3; δ = 1.84 methacrylate CH_2; δ = 1.02 methacrylate CH_3. ^{13}C NMR (D_2O): δ = 187.6, C═O; δ = 69.7, MPEG CH_2; δ = 57.1−51.5, quaternary carbon; δ = 47.1−46.2, methacrylate CH_2; δ = 20.4−17.5, methacrylate CH_3.

Sample Preparation. PMA-*g*-MPEG samples were prepared at 5 wt % in D_2O for structural characterization. Samples for T_2 NMR, PGSE NMR, and dynamic light scattering measurements were prepared in the dilute concentration regime at 0.1 wt % in 0.1 M NaCl D_2O by direct dissolution. Samples for potentiometric titration were prepared at 0.1 wt % by direct dissolution. pH or pD was adjusted by addition of less than 0.005 volume fraction 1.0 M NaOD, NaOH, DCl, or HCl. The samples were allowed to equilibrate for at least 48 h prior to measurements.

Potentiometric Titration. The dissociation behavior was monitored using an Orion 950 titration system fitted with a Ross Sure-Flow series pH electrode, standardized with Fisher Scientific Certified buffers at pH 4.01 and pH 10.01 prior to each titration. The polymer concentration was 0.10 wt %, and aqueous NaOH and HCl were used as titrants, at the same ionic strength with the polymer solution. All polymer samples were completely ionized polymer below pH 9.0, and each solution was not titrated below pH 5.0. Therefore, no ionic correction was needed.[32]

The solution pH was raised above pH 11 with aqueous NaOH and titrated to precipitation with 0.1 N HCl for each copolymer, allowing an equilibration time of 5 min per point. The degree of ionization, α, was calculated at 1.000 using a three-point second-derivative method for determination of inflection points.

***T*$_2$ NMR Measurements.** T_2 NMR measurements were performed using a standard Carr−Purcell/Meiboom−Gill (CPMG) pulse sequence ($90°_x-\tau-180°_y-\tau-$acq) with a Bruker 300 MHz spectrometer at 298 K. At least 50 measurements were obtained for each sample, using the following parameters: 90° pulse width (8.7 μs), echo delay (0−1.576 s), recycle delay (10 s), acquisition time (2 s). Between 16 and 64 transients were signal-averaged at each echo delay. The MPEG backbone signal was used for T_2 calculations.

PGSE NMR Diffusion Measurements. Self-diffusion measurements were performed using a Varian Standards broadband switchable probe with pulsed-field gradients (Varian Scientific) with a Mercury Innova 500 MHz spectrometer at 298 K by monitoring the signal attenuation of the methylene $-OCH_2CH_2-$MPEG peak. A standard pulsed gradient spin echo (PGSE) sequence utilized the following parameters: 90° pulse width (10.8 μs), acquisition time (1 s), recycle delay (10 s), mixing time (300 ms), and gradient duration (2−2.5 ms). The gradient amplitude G was calibrated using a deionized water ampule standard and adjusted to values ranging from 50 and 100 G/cm in each experiment, depending on sample pD, to yield at least 80% signal attenuation. The spectral width was set to 10 kHz and exponential line broadening set to 0.5 Hz. Between 16 and 256 transients were signal-averaged at each gradient level. The MPEG backbone signal presented the strongest resonance intensity, and its signal was used in PGSE calculations.

Dynamic Light Scattering. Dynamic light scattering was performed using a Brookhaven Instruments 128-channel BI-2030 AT digital correlator with a Spectra Physics He−Ne laser operating at 632.8 nm. The time-correlated signal decay was analyzed using CONTIN Laplace inversion routine to yield the polymer hydrodynamic diameter. All solutions were filtered through Whatman 1.0 μm polysulfone syringe filter. At least 10 measurements per sample were performed.

Scheme 1. Preparation of Poly(methacrylic acid)-*g*-poly(ethylene glycol)

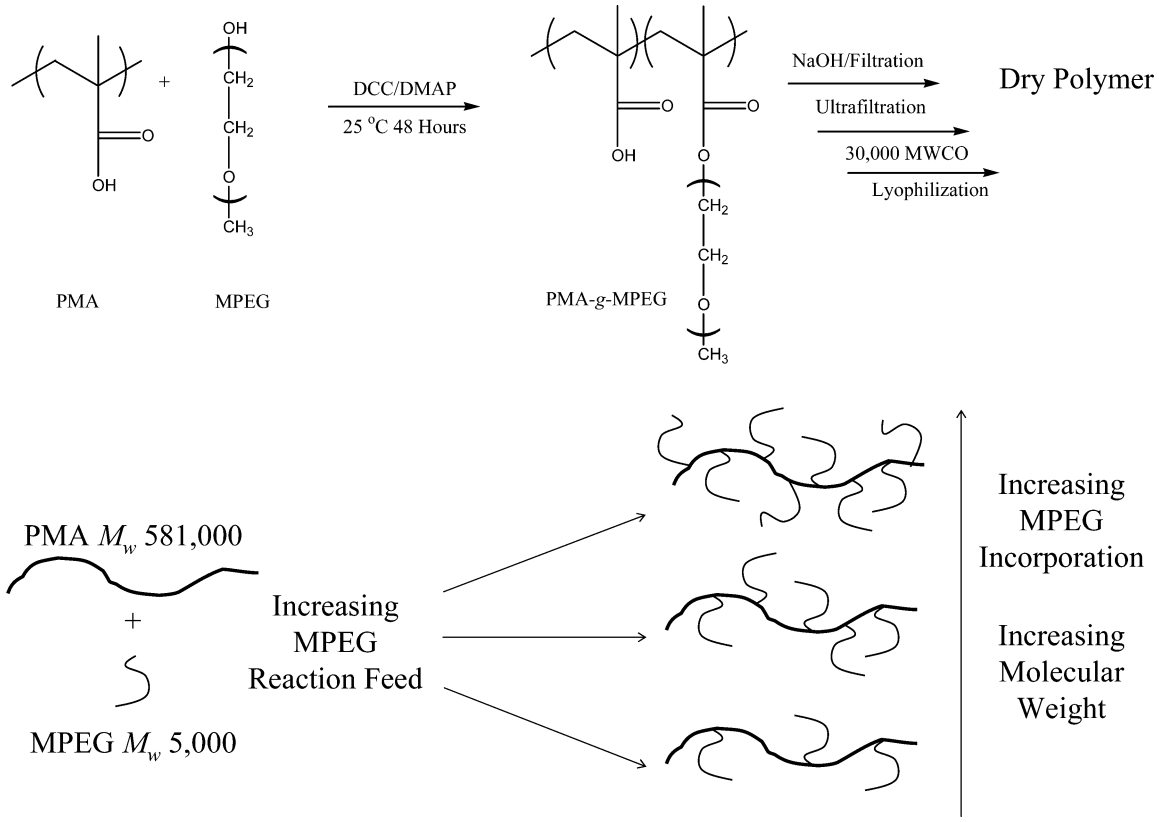

Classical Light Scattering. Classical light scattering (CLS) measurements were obtained using a Wyatt DAWN DSP multiangle laser light scattering detector in microbatch mode. The system was calibrated using toluene and normalized with bovine serum albumin (BSA) in an eluent of 0.5 M NaCl and 0.1 wt % NaN_3. All concentrations for each polymer sample were filtered with 0.1 μm Millipore syringe filters and injected with a syringe pump at a flow rate of 0.25 mL/min. Data were processed using ASTRA version 4.90.07.

Results and Discussion

Polymer Series Syntheses. A series of poly(methacrylic acid) polymers incorporating poly(ethylene glycol) grafts were synthesized by coupling monohydroxy monomethyl poly(ethylene glycol) to poly(methacrylic acid) in DMSO (Scheme 1). The molar MPEG incorporation was controlled by adjusting the MPEG/PMA ratio in the reaction mixture. All PMA-*g*-MPEG copolymers were synthesized using PMA prepared from the same methacrylic acid polymerization, therefore the molar incorporation and final copolymer molecular weight were dependent on the MPEG incorporation.

The final copolymer molecular weight was calculated from ^{1}H NMR analysis of the PMA-*g*-MPEG, as shown in Figure 1. The MPEG proton region ($\delta = 3.0-4.2$) and the methacrylate backbone region ($\delta = 0-2.5$) were integrated to determine the ratio of incorporated methacrylic acid to incorporated ethylene glycol (acid/base ratio), taking into account the contribution of the MPEG−methacrylate headgroup in the methacrylate backbone portion utilizing eq 1.

$$R = \frac{P_{EG}DP_{EG}A_{MA} - P_{MA}A_{EG}}{A_{EG}P_{MA}DP_{EG}} \quad (1)$$

where R is the incorporated ratio of methacrylic acid repeat units to ethylene glycol repeat units, P is the number of protons per repeat unit contributing to the ^{1}H resonance, DP is the degree of polymerization, and A is the integrated area of each section ($\delta = 3.0-4.2$ and $\delta = 0-2.5$). MA denotes the methacrylate portion of both MPEG−methacrylate and methacrylic acid ($-CH_2-C(CH_3)-$), and EG denotes ethylene glycol ($-CH_2CH_2O-$). For the current PMA-*g*-MPEG copolymers, $P_{EG} = 4$, $DP_{EG} = 114$, and $P_{MA} = 5$.

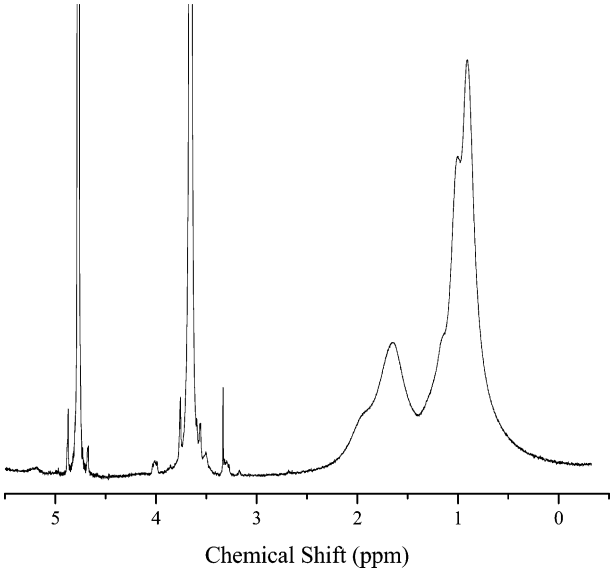

Figure 1. Typical ^{1}H NMR spectrum of PMA-*g*-MPEG in D_2O. $\delta = 4.77$, HOD; $\delta = 4.01$, ester CH_2; $\delta = 3.65$, MPEG $-CH_2-$; $\delta = 3.32$, MPEG $-CH_3$; $\delta = 1.84$ methacrylate CH_2; $\delta = 0.92$ methacrylate $-CH_3$.

Three copolymer samples were selected for study, representing a range of acid/base ratios: PMA-*g*-MPEG 0.6, 0.7, and 1.0 and are presented in Table 1. Data for

Table 1. PMA-*g*-MPEG Incorporation Data, Calculated from ^{1}H NMR

	reaction feed			incorporation				mol wt × 10^{-5}			copolymer composition			
coplymer	EG/ MAA	MAA/ MPEG	MPEG/ PMA	EG/ MAA	MAA/ MPEG	MPEG/ PMA	graft eff (%)	M_{MPEG}	M_n[a]	M_w[b]	X_{MAA}	X_{EG}	W_{MAA}	W_{EG}
PMA homo								0		5.8	1.00	0.00	1.00	0.00
PMA-*g* -MPEG 0.6	3.00	37.9	142	0.6	200	26	18.5	1.3	7.1	8.0	0.64	0.36	0.82	0.18
PMA-*g* -MPEG 0.7	4.00	28.4	189	0.7	170	32	16.8	1.6	7.4	8.3	0.60	0.40	0.79	0.22
PMA-*g* -MPEG 1.0	5.00	22.7	237	1.0	120	46	19.3	2.3	8.1	14.7	0.51	0.49	0.72	0.28
PMA-*mix* -MPEG	1.00	113.6	47.3					0		5.8	0.50	0.50	0.71	0.29

[a] Calculated from ^{1}H NMR. [b] Calculated from static light scattering.

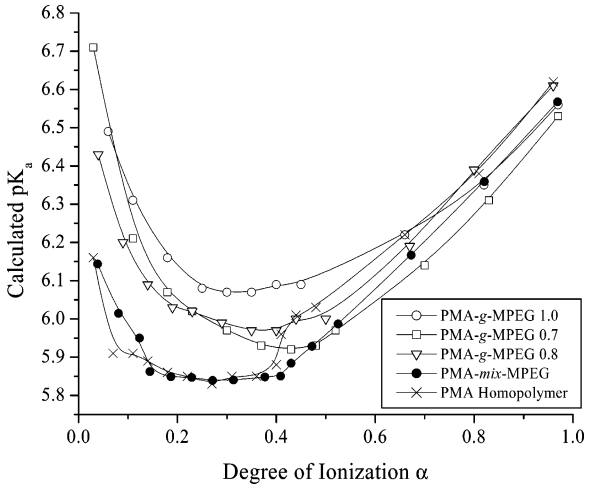

Figure 2. 0.1 wt % in 0.1 M NaCl/H_2O. The apparent pK_a is calculated as a function of degree of ionization α. The characteristic upturn with decreasing α exhibited for PMA homopolymer and PMA/MPEG control mixture is greatly enhanced for PMA-*g*-MPEG copolymers. This phenomenon indicates higher acidic proton binding potential resulting from the for PMA hydrogen-bonding interaction with tethered MPEG in copolymers at low ionization.

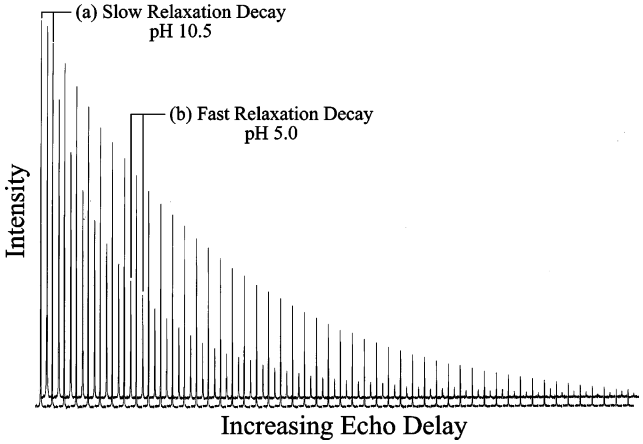

Figure 3. Representative MPEG proton T_2 experiment, 0.1 wt % in 0.1 M NaCl/D_2O. (a) PMA-*g*-MPEG, pH 10.5. (b) PMA-*g*-MPEG, pH 5.0.

a control mixture of PMA homopolymer and MPEG, mixed in a 1:1 stoichiometry of methacrylic acid to ethylene glycol units, are also presented.

The final molecular weight (an approximation of M_n) for each sample was calculated utilizing NMR data. The backbone chain length remains approximately constant for all samples at approximately 5400 residues, and the increase in molecular weight is due to only the grafted MPEG chains. Molecular weight (M_w) data obtained from static light scattering are also presented and show reasonable agreement with the M_n approximation. The graft copolymer with the highest MPEG incorporation (PMA-*g*-MPEG 1.0) produced a slightly higher M_w than anticipated from the M_n results, likely arising from a small fraction of difunctional MPEG species.

Potentiometric Titrations. Figure 2 shows the apparent pK_a values as a function of the degree of ionization, α, calculated from eq 2 and utilizing experimental values of pH deteremined from potentiometry.[32]

$$pK_a = pH + \log\left(\frac{1-\alpha}{\alpha}\right) \qquad (2)$$

The pK_a values of polyelectrolytes which do not exhibit conformational transitions during ionization increase monotonically as a function of degree of ionization.[32] The characteristic upturn exhibited for PMA and PMA-*mix*-MPEG with decreasing α arises from an additional dissociation energy contribution due to the PMA coil−globule conformational transition.[32] This upturn for PMA is greatly exaggerated for PMA-*g*-MPEG copolymers, indicating higher acidic proton binding potential resulting from the PMA hydrogen-bonding interaction with tethered MPEG in copolymers at low ionization. The apparent pK_a increases with MPEG incorporation at $\alpha < 0.4$.

Deviations from the PMA plot provide insight into the dissociation behavior of PMA-*g*-MPEG copolymers. The curve inflection is apparent for PMA and PMA-*mix*-MPEG, corresponding to the coil−globule transition of PMA in aqueous solutions.[32] The absence of an inflection point for the PMA-*g*-MPEG samples suggests a broadening in the normally sharp transition.

NMR T_2 Measurements. Spin−spin relaxation involves the transfer of energy among the precessing protons, resulting in signal loss from spin dephasing and line broadening.[33] The T_2 relaxation for polymers is heavily influenced by the local rigidity, and polymeric protons constrained locally exhibit faster T_2 relaxations than identical protons in a less constrained environment. Consequently, T_2 relaxation measurements are a convenient method of probing the local flexibility of polymeric segments. The high flexibility of MPEG ether bonds provides characteristically long T_2 relaxations in the absence of local restrictions, resulting in narrow ^{1}H NMR resonance. PMA backbone protons experience faster spin−spin relaxations resulting from local flexibility constraints along the high molecular weight, hydrophobic backbone. Consequently, the MPEG resonances at 3.65 ppm were examined in these relaxation experiments.

Figure 3 depicts the MPEG portion of the ^{1}H NMR spectrum for representative T_2 decays for PMA-*g*-MPEG. Each peak is the MPEG signal from the ^{1}H spectrum obtained by incrementally increasing the echo delay (τ) from 0 to 1576 ms. From these data, the apparent T_2 decay is calculated by nonexponential curve

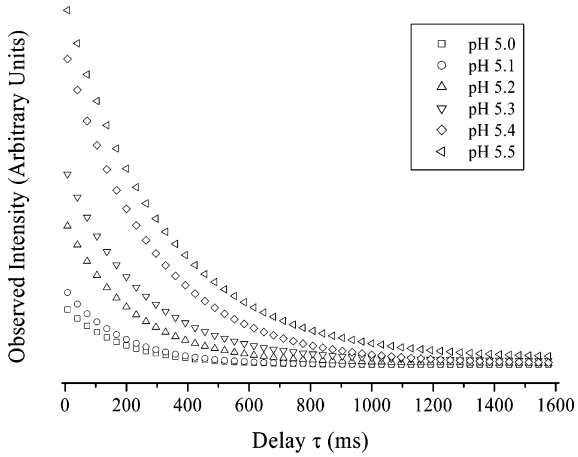

Figure 4. Typcial intensity decay for PMA-*g*-MPEG copolymers, 0.1 wt % in 0.1 M NaCl/D_2O.

fitting using eq 3.[34]

$$\ln\left(\frac{I_\tau}{I_0}\right) = \frac{-2\tau}{T_2} \tag{3}$$

The MPEG intensity decays at a slower rate for series a than series b, indicating higher MPEG side-chain conformational freedom at pH 10.5 than at pH 5.0. This is consistent with the degree of MPEG hydrogen bonding with the PMA backbone, at these pH values. Thus, the spin−spin decay rate increase may be used to monitor hydrogen-bond formation between PMA backbone and MPEG grafts as a function of PMA ionization.

The continual increase in conformational restriction throughout the pH range of 5.0−5.5 is illustrated in Figure 4. The normalized intensity of each MPEG signal observed after the CPMG sequence is plotted as a function of echo delay for each pH. PMA ionization increases with pH, and thus the time for signal decay increases, indicating decreased conformational restrictions of MPEG. Thus, the variation in MPEG T_2 with pH is a method of probing the chain restrictions of pH for each PMA-*g*-PEG copolymer and the control mixture.

Figure 5a illustrates that MPEG spin−spin relaxations are essentially unchanged for the PMA-*g*-MPEG and control mixture in region 2. Changes in ionization of the PMA portion do not affect the MPEG conformation across this pH range. However, the abrupt downturn in region 1 at lower PMA ionization is evident in Figure 5a and enlarged in Figure 5b.

The MPEG copolymer side chains exhibit relaxation downturn at ∼pH 5.6−5.7. Further decreases in pH result in continued decrease of the observed MPEG spin−spin relaxations for the copolymers, lowering the observed T_2 value from ∼450 ms to well below 200 ms. These data suggest that the onset of intramolecular hydrogen-bond formation for PMA-*g*-MPEG copolymers occurs at pH 5.6−5.7, corresponding to a degree of ionization of $\alpha = 0.30-0.35$. Further complexation continues to pH 5.0 (ionization $\alpha = 0$) as the MPEG copolymer side chains experience increasing restrictions to their conformational freedom throughout this range.

In sharp contrast to the above, MPEG T_2 relaxations in the control mixture are not affected by PMA ionization changes across the entire pH range, indicating no hydrogen-bond formation. The mixture is a compositional analogue to the PMA-*g*-MPEG 1.0 sample without covalent MPEG−methacrylate bonds, and it is reasonable to attribute the enhancement in hydrogen-bond formation of the PMA-*g*-MPEG series to the proximity of the two chain segments. While the protic dissociation of PMA homopolymer is identical to that of PMA mixtures across the pH range 5.0−10.5 ($\alpha = 0.15-1.0$), previous reports indicate that MPEG interactions with PMA only occur for ionization levels below $\alpha = 0.10$ (pH < 4.85), at solution pH outside the range of these experiments.

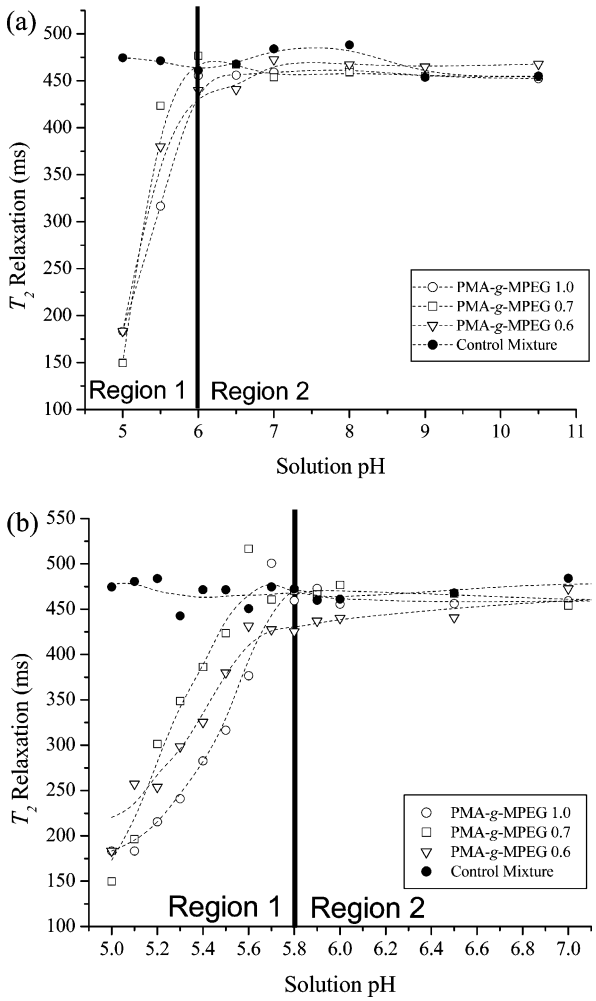

Figure 5. T_2 relaxations for MPEG protons in PMA-*g*-MPEG copolymers and control mixture, 0.1 wt % in 0.1 M NaCl/D_2O. (a) pH 5.0−10.5; (b) pH 5.0−6.0: open circles. PMA-*g*-MPEG 1.0; open squares, PMA-*g*-MPEG 0.7; open triangles, PMA-*g*-MPEG 0.6; closed circles, control mixture.

It is important to note that MPEG tethered to a PMA backbone can be considered either complexed with PMA or uncomplexed. When exchange between the two states is slower than the CPMG pulse echo delay, the observed T_2 relaxation is determined by the fractional contribution, ρ, of each MPEG state A and B, using eq 4.[35]

$$T_{2,\mathrm{obs}} = \rho_A T_{2,A} + \rho_B T_{2,B} \tag{4}$$

Systems with multiple populations having different T_2 relaxation times exhibit nonlinear dependence of $\ln(I/I_0)$ with decay time. A representative example for the current PMA-*g*-MPEG copolymers is illustrated in Figure 6. The curved decays transition to linear decays in region 1 for all copolymer systems, indicating the presence of at least two populations with different T_2 relaxation times. The fractions of unbound and bound MPEG chains were calculated according to eq 4. $T_{2,\mathrm{unbound}}$,

Table 2. Calculation of MPEG Participating in Hydrogen Bonding with PMA Backbone from T_2 Measurements

	PMA-*g*-MPEG 1.0			PMA-*g*-MPEG 0.7			PMA-*g*-MPEG 0.6			PMA-*mix*-MPEG		
pH	(ms)	ρ_A	ρ_B	(ms)	ρ_A	ρ_B	(ms)	ρ_A	ρ_B	(ms)	ρ_A	ρ_B
5.00	183	0.70	0.30	150	0.79	0.21	183	0.70	0.30	475	−0.04	1.04
5.10	183	0.70	0.30	196	0.67	0.33	257	0.51	0.49	481	−0.06	1.06
5.20	216	0.62	0.38	301	0.40	0.60	254	0.52	0.48	484	−0.07	1.07
5.30	241	0.55	0.45	349	0.28	0.72	299	0.41	0.59	443	0.04	0.96
5.40	283	0.45	0.55	386	0.18	0.82	325	0.34	0.66	472	−0.03	1.03
5.50	317	0.36	0.64	423	0.09	0.91	380	0.20	0.80	471	−0.03	1.03
5.60	377	0.21	0.79	517	−0.15	1.15	431	0.07	0.93	451	0.02	0.98
5.70	501	−0.11	1.11	461	−0.01	1.01	428	0.08	0.92	475	−0.04	1.04
5.80	460	0.00	1.00	471	−0.03	1.03	425	0.08	0.92	473	−0.04	1.04
5.90	473	−0.04	1.04	466	−0.02	1.02	437	0.05	0.95	460	0.00	1.00
6.00	456	0.01	0.99	477	−0.05	1.05	440	0.05	0.95	461	−0.01	1.01
6.50	456	0.01	0.99	467	−0.02	1.02	441	0.04	0.96	468	−0.03	1.03
7.00	459	0.00	1.00	454	0.01	0.99	473	−0.04	1.04	484	−0.07	1.07
8.00	463	−0.01	1.01	459	0.00	1.00	467	−0.02	1.02	488	−0.08	1.08
9.00	454	0.01	0.99	455	0.01	0.99	465	−0.02	1.02	454	0.01	0.99
10.50	452	0.01	0.99	454	0.01	0.99	468	−0.02	1.02	455	0.01	0.99

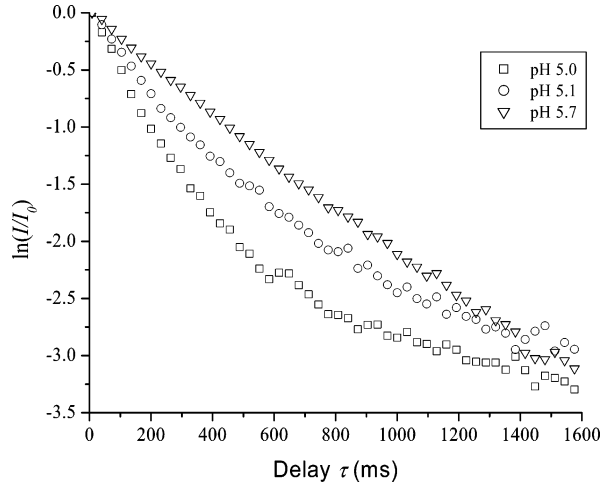

Figure 6. Nonlinearity of spin−spin relaxation time measurements for PMA-*g*-MPEG copolymer at three pH conditions: squares, pH 5.0; circles, pH 5.1; triangles, pH 5.7. Nonlinear curves indicate the presence of more than one population with different T_2 relaxation times.

the T_2 relaxation of the tethered MPEG chains not participating in hydrogen bonding, was determined by the average observed T_2 value at pH 10.5 (458 ms average) for all copolymer systems. Spin−spin relaxation is not affected by molecular weight differences below the critical overlap concentration, and $T_{2,\text{bound}}$, the T_2 relaxation of tethered MPEG participating in hydrogen bonding, was approximated as ∼65 ms by using the observed T_2 of MPEG M_w 100 000 in the presence of PMA at a 5:1 stoichiometric excess of PMA at $\alpha = 0$. The T_2 relaxation of the same system at pH 10.5 was also measured at 460 ms. The fraction of side-chain MPEG participating in hydrogen bonding decreases from ∼0.7 to ∼0.0 in region 1 and remains constant in region 2.

The fraction of tethered MPEG chains participating in hydrogen bonding with the PMA backbone at pH 5.0 was calculated as ∼70% for all copolymer systems in this study. The number of available hydrogen-bonding sites on PMA is reduced by increasing the ionization of the PMA chain with system pH. Ionized PMA moieties are no longer capable of hydrogen-bond formation with MPEG, and the fraction of bound MPEG decreases to a certain limiting pH ∼5.7. Further increases in ionization do not affect the participation of tethered MPEG chains in the formation of hydrogen bonds with PMA. These data contrast earlier findings[36] of PMA mixtures with MPEG, which generally do not occur above 0.1 ionization.

There is no obvious trend in the hydrogen-bond formation capability of PMA-*g*-MPEG copolymers with different levels of MPEG incorporation. Formation of hydrogen-bonding polymer pairs is a sterically limited process, and it seems likely that lower incorporation of MPEG grafts would allow for higher levels of MPEG participating in hydrogen-bond formation with PMA backbone. However, these results indicate that the participation of MPEG is limited only by the ionization of the backbone, at least through the range of MPEG incorporations in this study.

PGSE NMR Diffusion Measurements. The Stejskal−Tanner equation[37] (eq 5) relates nuclear magnetic resonance signal attenuation to gradient pulse strength.

$$\frac{I}{I_0} = \exp\left[-(\gamma G\delta)^2\left(\Delta - \frac{\delta}{3}\right)D\right] \qquad (5)$$

I is the resonance intensity, γ is the gyromagnetic ratio of protons (2.67515×10^4 G^{-1} s^{-1}), G is the gradient strength, δ is the gradient duration, Δ is the separation between the gradient pulses, and D is the diffusion coefficient. Incremental variations in G at a constant Δ allow determination of an apparent diffusion constant by monitoring observed signal intensity after the PGSE sequence. Signal attenuation data from water contained in an NMR ampule are shown in Figure 7. The plot of $\ln(I/I_0)$ vs G^2 affords a linear relationship, common for systems with a single-diffusing species. The diffusion constant is extracted from the slope.

The observed dependence of $\ln(I/I_0)$ on $(\gamma G\delta)^2(\Delta - \delta/3)$ for the copolymer systems is markedly nonlinear, as shown in Figure 8. Nonlinear attenuation curves suggest restricted diffusion, multiple diffusing species, or a dispersion of diffusion coefficients.[34] Given that the systems were prepared below the critical overlap concentration, restricted diffusion is unlikely. While multiple diffusing species have been observed for other synthetic copolymers involving free-radically synthesized copolymers containing separate fractions of high and low comonomer incorporation, it is unlikely that the conditions for the present synthesis would cause such incorporation inconsistency; indeed, dynamic light scattering confirms the presence of one diffusing species. Since the synthesized PMA backbone was prepared by

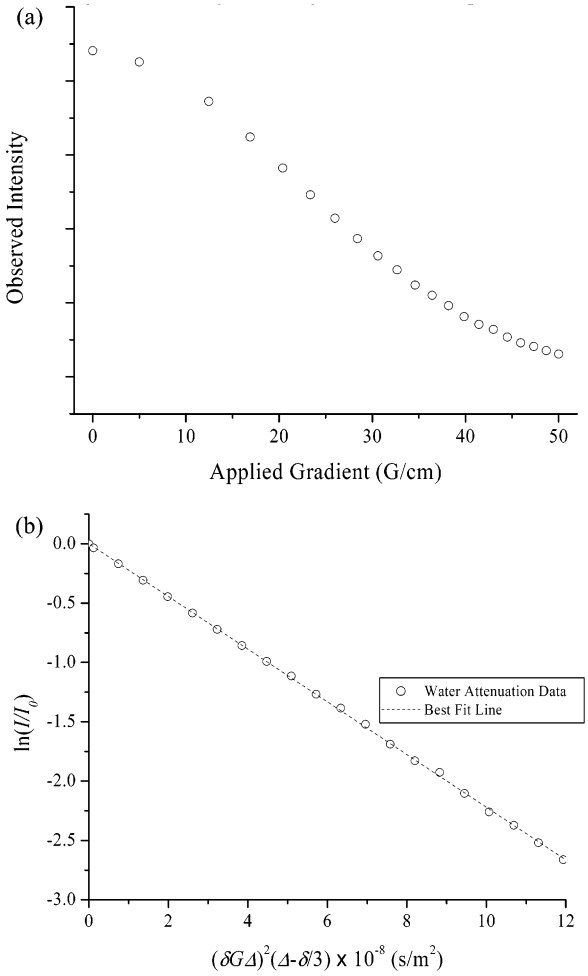

Figure 7. PGSE diffusion data for water standard: (a) observed signal intensity as a function of gradient strength; (b) signal attenuation plot with best fit line.

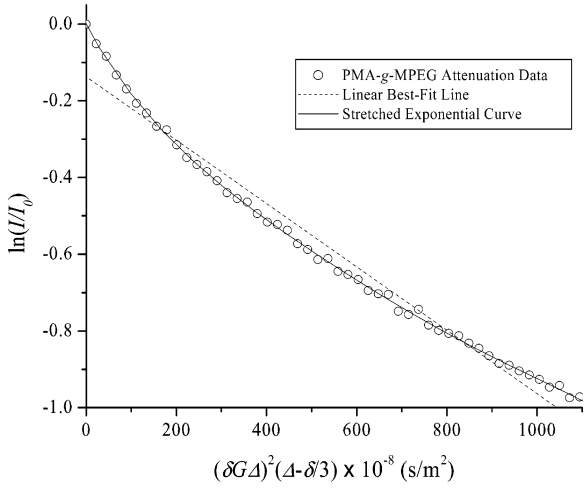

Figure 8. Representative PGSE attenuation curve for PMA-*g*-MPEG copolymers, 0.1 wt % in 0.1 M NaCl/D_2O: open circles, observed data; dotted line, linear fit to eq 5; solid line, stretched exponential fit to eq 6.

classical free-radical polymerization, it should, therefore, exhibit a broader diffusion coefficient than a monodisperse diffusing species. For this case, eq 5 may be modified with a stretched exponential. The resulting relationship (eq 6) adequately describes the effective diffusion coefficient (D_e) from PGSE data obtained from polydisperse systems.[34]

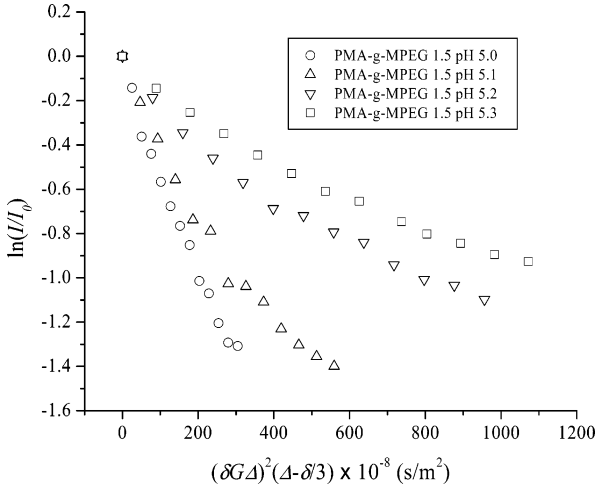

Figure 9. Typical intensity delays observed for the same PMA-*g*-MPEG (0.7) copolymer at several pH, 0.1 wt % in 0.1 M NaCl/D_2O: circles, pH 5.0; up triangles, pH 5.1; down triangles, pH 5.2; squares, pH 5.4. The coefficient of diffusion D_e and distribution coefficient β are extracted from the data.

$$\frac{I}{I_0} = \exp\left(-\left[(\gamma G\delta)^2\left(\Delta - \frac{\delta}{3}\right)D_e\right]^{\beta}\right) \qquad (6)$$

The measure of the width of the distribution coefficient is contained in the parameter β, which varies from zero to one. For monodisperse samples, $\beta = 1$ and eq 6 reduces to eq 5.[34]

The signal attenuations of PMA-*g*-MPEG of a representative pH range 5.0−5.4 are depicted in Figure 9. The slope of $\ln(I/I_0)$ vs $(\gamma G\delta)^2(\Delta - \delta/3)$ curves are proportional to $-D$, with sharper slopes indicating higher diffusion constants. The diffusion rate is determined by coil size, and a change in diffusion rate indicates a change in coil size. In this representative example, the slope decreases from pH 5.0 to 5.4 (Figure 9), indicating faster diffusion resulting from smaller coil size at pH 5.0 and slower diffusion from larger coil size at pH 5.4.

The effective diffusion coefficient was calculated from eq 6 at each pH for the three copolymer systems. The diffusion constant of untethered MPEG was also calculated for the control mixture. Figure 10a depicts the dependence of D_e on solution pH. The distribution coefficient β was ∼0.70−0.85 for all systems, indicating a reasonably monodisperse distribution of diffusing species.[34] The copolymers exhibit negligible changes in diffusion rate above pH 6.0 and a marked increase below pH 6.0. Starting from pH 5.0, the coils expand to a certain size that does not change upon further increase in pH. The enlarged region 1 from pH 5.0−7.0 in Figure 10b shows that a transition in coil size occurs at pH 5.6−5.8 for each copolymer, approximately the same range as the transition in T_2 relaxation times.

The rate of self-diffusion for all PMA-*g*-MPEG copolymers across the entire pH range decreases with increasing MPEG incorporation. The PMA backbone is a constant length for all copolymers, and the increase in molecular weight occurring from increasing the MPEG incorporation increases the coil hydrodynamic volume, decreasing the observed D_e.

The untethered MPEG chains in the PMA-*mix*-MPEG systems do not exhibit change in D_e across the entire pH range. PMA potentially limits self-diffusion by

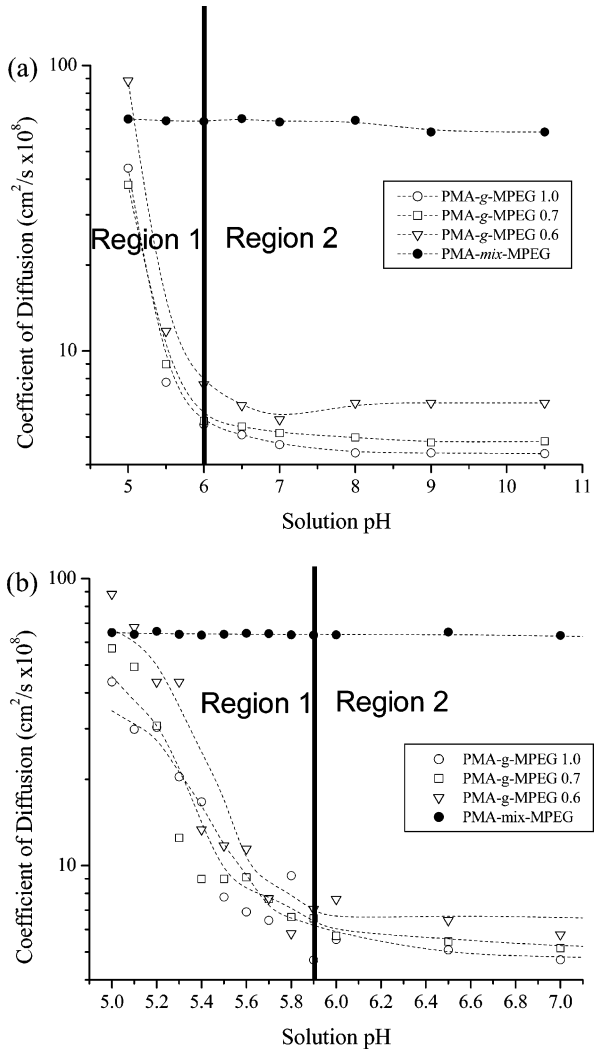

Figure 10. Effective diffusion coefficients (D_e) for PMA-*g*-MPEG copolymers and PMA-*mix*-MPEG mixture, 0.1 wt % in 0.1 M NaCl/D_2O. The diffusion coefficients are approximately the same for all copolymers above pH 6.0 and increase as the pH is lowered to pH 5.0, corresponding to a change in coil size from expanded conformation at high pH to collapsed conformation at low pH. (a) The change of D_e across the entire range of pH; (b) enlarged portion of (a) containing only pH 5.0−7.0.

forming an interpolymer hydrogen-bonding complex at low pH. The formation of a complex from participating PMA homopolymers and MPEG homopolymers occurs readily PMA ionization of <0.10. However, at solution pH 5.0, the PMA homopolymer chain ionization in 0.1 M NaCl is calculated at ~0.14 (data not shown), too high for formation of intermolecular complexes with the untethered MPEG. The diffusion rate of the free MPEG is not affected by changes in ionization of PMA across the pH range in this study, indicating no participation of untethered MPEG chains in the formation of hydrogen-bonding interpolymer complexes.

These diffusion data appear to indicate that the coil size of PMA-*g*-MPEG copolymers at pH 5.0 is approximately the same as untethered MPEG in solution. Given the molecular weight differences between PMA-*g*-MPEG (700 000−800 000 g/mol) and the free MPEG (5000 g/mol), this does not seem reasonable.

One possible explanation that might be put forward for the D_e observations is that diffusion values are actually due to a fraction of hydrolyzed MPEG, free in solution and no longer tethered to the PMA backbone.

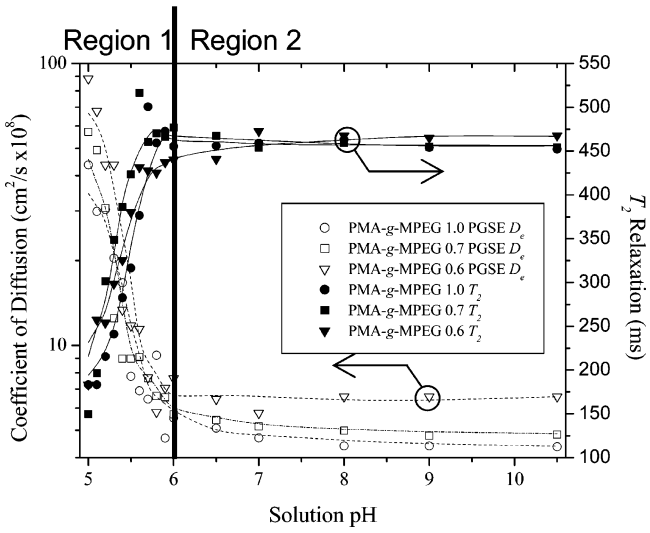

Figure 11. T_2 (solid lines) relaxation and PGSE D_e (dashed lines) of PMA-*g*-MPEG copolymers, 0.1 wt % in 0.1 M NaCl/D_2O: circles, PMA-*g*-MPEG 1.0; squares, PMA-*g*-MPEG 0.7; triangles, PMA-*g*-MPEG 0.6.

However, the T_2 relaxation data should be similar to the PMA-*mix*-MPEG solutions in this scenario. Given the significantly shorter T_2 relaxation for PMA-*g*-MPEG at lower pH as compared to PMA-*mix*-MPEG at all pH values, the hydrolyzed MPEG proposal does not agree with T_2 observations for the PMA-*g*-MPEG systems at low pH.

We suggest another explanation. The PMA-*g*-MPEGs are high molecular weight polymers and require a significant mixing time (300 ms) to manifest reasonable signal decay at maximum gradient strength (100 G/cm). The unusually long T_2 at high ionization is drastically shortened at low ionization, and the decreased MPEG hydration affects a significant signal loss at low ionizations during mixing. Higher gradient strengths (beyond the capability of our gradient probe) are necessary to decrease mixing time and provide realistic diffusion estimates at low ionizations. Therefore, we do not believe the data at low pH can be justified.

The simultaneous changes in T_2 relaxation of the tethered MPEG and PGSE-determined D_e of the PMA-*g*-MPEG copolymers are shown in Figure 11. Local increases in MPEG rigidity in region 1 are accompanied by decreases in the total hydrodynamic volume of the respective copolymers.

The spin−spin relaxation times for PMA protons are fast on the time scale of the PGSE sequence, leading to line broadening and signal loss. The utility of the pulsed-gradient technique under these gradient strengths is, therefore, limited to species with relatively long T_2 relaxations, as compared to the mixing time. The signal of the PMA protons immediately disappears as gradient strength increases, negating the possibility of the direct measurement of PMA or PMA-based copolymers in solution.

Dynamic Light Scattering Measurements. Dynamic light scattering was employed to overcome the above limitations of the PGSE method and to serve as an alternate route to measure diffusion of PMA-*g*-MPEG copolymers. Light scattering data were obtained using polymer solutions. D_2O solutions previously prepared for PGSE and T_2 measurements provide nearly identical results, indicating negligible effect of D_2O on diffusion properties.

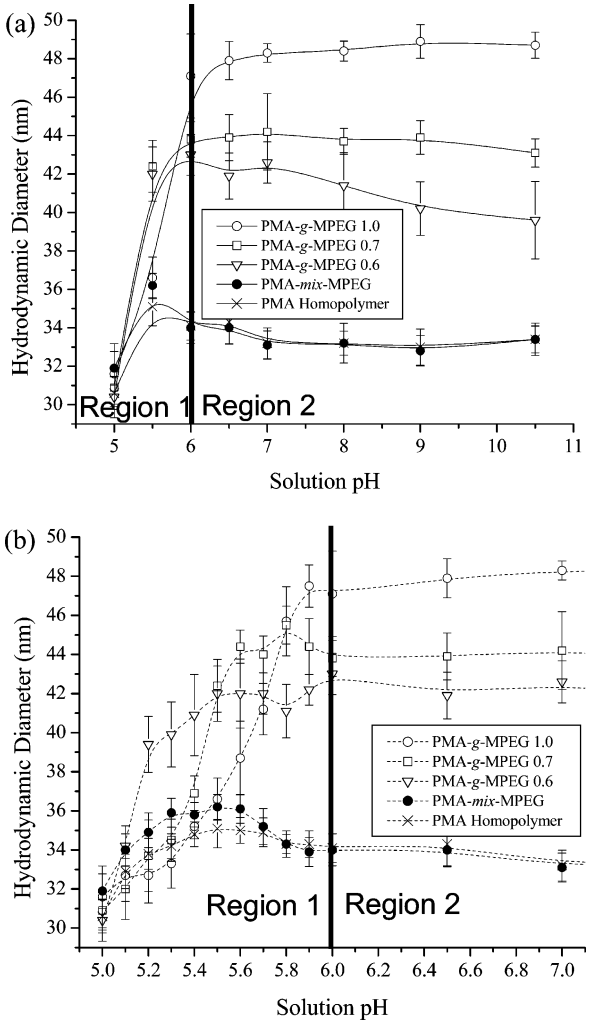

Figure 12. Hydrodynamic diameter from dynamic light scattering data for PMA-*g*-MPEG copolymers and PMA-*mix*-MPEG control mixture, 0.1 wt % in 0.1 M NaCl: (a) change of D_h across the entire range of pH; (b) enlarged portion of (a) containing only pH 5.0−7.0.

The change in hydrodynamic coil size with pH is depicted in Figure 12a, with the enlarged region of the coil transition in Figure 12b. PMA and PMA-*mix*-MPEG exhibit coil expansion from ∼30 to 33 nm, while the PMA-*g*-MPEG 1.0, 0.7, and 0.6 copolymers expand from ∼32 nm to 48, 44, and 39 nm, respectively.

The enlarged region 1 in Figure 12b shows that a transition in coil size occurs between pH 5.0 and 5.8 for each copolymer, approximately the same range as the transition in T_2 and D_e.

The responses exhibited by the PMA homopolymer and PMA-*mix*-MPEG are effectively identical, indicating that untethered MPEG does not participate in the coil collapse of PMA, in agreement with T_2 and D_e data. The PMA-*g*-MPEG coils in region 2 are 6−16 nm larger than the unmodified PMA, while at pH 5.0 are approximately the same size, despite having a significantly higher molecular weight than PMA. Clearly, the PMA-*g*-MPEG copolymers experience a more significant enhancement in hydrodynamic volume change across this pH range than the unmodified PMA starting polymer. The coil sizes of each sample follow the trend observed in the PGSE measurements: PMA-*g*-MPEG 1.0 > PMA-*g*-MPEG 0.7 > PMA-*g*-MPEG 0.6 > PMA-*mix*-MPEG = PMA homopolymer. Each MPEG side chain has an associated hydrodynamic volume, which cannot be ignored. Under conditions of sufficient PMA ionization (region 2), tethered MPEG does not form hydrogen bonds with PMA and exists as a side coil of polymer and associated solvent. The PMA backbone adopts a more expanded conformation to allow room for the side chains, and the copolymer hydrodynamic volume increases as a function of MPEG incorporation.

The copolymer hydrodynamic diameters at pH 5.0 (32−33 nm) are approximately the same as the PMA homopolymer (30−31 nm). The dynamic light scattering measurements yield a more realistic size than that from the PGSE data at low pH.

Despite having significantly higher molecular weight, the coil sizes of PMA-*g*-MPEG are approximately the same as that of the PMA homopolymer at low ionization. The coil size expansion observed in region 2, arising from the swollen MPEG side chains, has decreased, if not disappeared completely. T_2 and potentiometric titration measurements indicate that in region 1 MPEG participates in hydrogen-bonding complexes with PMA. This participation frees each MPEG side coil of associated solvent, allowing an enhanced PMA coil collapse with decreasing ionization. Further, PMA−MPEG hy-

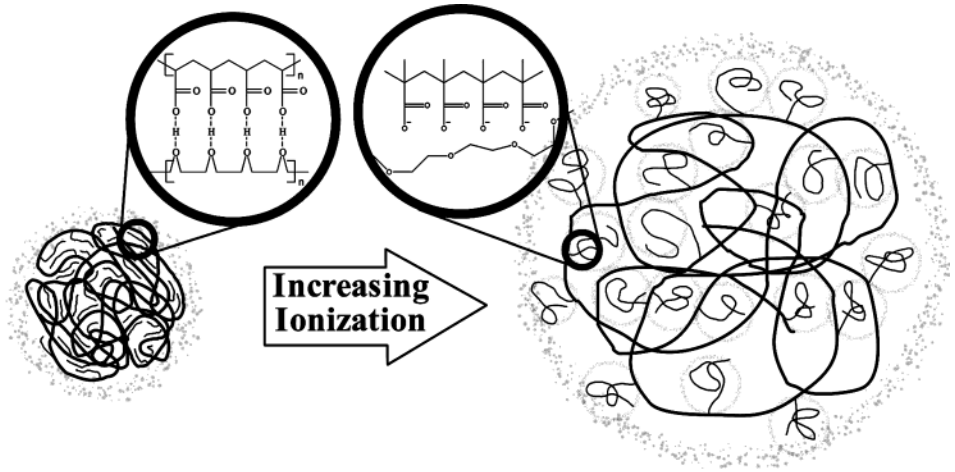

Figure 13. Schematic of PMA-*g*-MPEG coil expansion with increasing ionization. The presence of tethered MPEG chains has two effects on coil size of PMA-*g*-MPEG. At high ionization, the coil expands due to the added volume of the tethered MPEG and the increased PMA ionization. At low ionization, the tethered MPEG increases hydrophobic stabilization of the globule, dehydrating the polymer to a smaller hydrodynamic volume.

drogen-bonding complexes are hydrophobic and induce coil collapse at low pH.

Conclusions

Copolymers of poly(methacrylic acid) with varying molar quantities of poly(ethylene glycol) were successfully synthesized by a postpolymerization grafting reaction in organic media. Potentiometric titrations and T_2 relaxation measurements show an enhancement of hydrogen-bonding interaction between PMA and the tethered MPEG, which was not present across the same pH range for mixed PMA/MPEG analogues. The covalent attachment enhances the formation of hydrogen bonding for attached MPEG groups. The relative amounts of hydrogen-bonded MPEG were determined at each ionization level.

The self-diffusion properties of PMA-*g*-MPEG were probed with PGSE NMR and DLS techniques. The effect of covalently attached MPEG on the conformation of the PMA backbone is twofold. First, the PMA expands as the hydrophilic chains swell with solvent in region 2, affecting an overall expansion of PMA. Second, the MPEG forms hydrogen-bonding hydrophobic complexes in region 1, enhancing coil collapse and offsetting the inherent size arising from the overall molecular weight increase.

Acknowledgment. The authors thank the Department of Energy (DE-FC26-01BC15317) for financial support. Useful discussion with Yoshimitsu Uemura of Kagoshima University is gratefully acknowledged.

References and Notes

(1) Leobandung, W.; Ichikawa, H.; Fukumori, Y.; Peppas, N. A. *J. Appl. Polym. Sci.* **2001**, *87*, 1678−1684.
(2) Fevola, M. J.; Hester, R. D.; McCormick, C. L. *J. Polym. Sci., Part A: Polym. Chem.* **2003**, *41*, 560−568.
(3) Cowan, M. E.; Garner, C.; Hester, R. D.; McCormick, C. L. *J. Appl. Polym. Sci.* **2001**, *82*, 1222−1231.
(4) Cowan, M. E.; Hester, R. D.; McCormick, C. L. *J. Appl. Polym. Sci.* **2001**, *82*, 1211−1221.
(5) Armentrout, R. S.; McCormick, C. L. *Macromolecules* **2000**, *33*, 2944−2951.
(6) Huibers, P. D. T.; Bromberg, L. E.; Robinson, B. H.; Hatton, T. A. *Macromolecules* **1999**, *32*, 4889−4894.
(7) Zhang, J.; Peppas, N. A. *Macromolecules* **2000**, *33*, 102−107.
(8) Kim, C.; Lee, S. C.; Kwon, I. C.; Chung, H.; Jeong, S. Y. *Macromolecules* **2002**, *35*, 193−200.
(9) Nikolaeva, O.; Budtova, T.; Bobrova, N.; Bronnikov, S. *J. Macromol. Sci., Phys.* **2001**, *B40*, 539−552.
(10) Chatterjee, S. K.; Malhotra, A. *J. Macromol. Sci., Chem.* **1984**, *A21*, 765−773.
(11) Klier, J.; Scranton, A. B.; Peppas, N. A. *Macromolecules* **1990**, *23*, 4944−4949.
(12) Mathur, A. M.; Drescher, B.; Scranton, A. B.; Klier, J. *Nature (London)* **1998**, *392*, 367−370.
(13) Drescher, B.; Scranton, A. B.; Klier, J. *Polymer* **2001**, *42*, 49−58.
(14) Hemker, D. J.; Garza, V.; Frank, C. W. *Macromolecules* **1990**, *23*, 4411−4418.
(15) Bimendina, L. A.; Roganov, V. V.; Bekturov, E. A. *J. Polym. Sci., Polym. Symp.* **1974**, *44*, 65−74.
(16) Fredheim Guro, E.; Christensen Bjorn, E. *Biomacromolecules* **2003**, *4*, 232−239.
(17) de Jong, S. J.; De Smedt, S. C.; Wahls, M. W. C.; Demeester, J.; Kettenes-van den Bosch, J. J.; Hennink, W. E. *Macromolecules* **2000**, *33*, 3680−3686.
(18) Bednar, B.; Li, Z.; Huang, Y.; Chang, L. C. P.; Morawetz, H. *Macromolecules* **1985**, *18*, 1829−1833.
(19) Oyama, H. T.; Tang, W. T.; Frank, C. W. *Macromolecules* **1987**, *20*, 474−480.
(20) Lowman, A. M.; Peppas, N. A. *Macromolecules* **1997**, *30*, 4959−4965.
(21) Bednar, B.; Morawetz, H.; Shafer, J. A. *Macromolecules* **1984**, *17*, 1634−1636.
(22) Baranovsky, V. Y.; Shenkov, S. *J. Polym. Sci., Part A: Polym. Chem.* **1996**, *34*, 163−167.
(23) Song, T.; Goh, S. H.; Lee, S. Y. *Macromolecules* **2002**, *35*, 4133−4137.
(24) Huang, X. D.; Goh, S. H. *Macromolecules* **2000**, *33*, 8894−8897.
(25) Osada, Y.; Sato, M. *J. Polym. Sci., Polym. Lett. Ed.* **1976**, *14*, 129−134.
(26) Zeghal, M.; Auvray, L. *Europhys. Lett.* **1999**, *45*, 482−487.
(27) Philippova, O. E.; Starodubtzev, S. G. *J. Macromol. Sci., Pure Appl. Chem.* **1995**, *A32*, 1893−1902.
(28) Kim, B.; La Flamme, K.; Peppas, N. A. *J. Appl. Polym. Sci.* **2003**, *89*, 1606−1613.
(29) Torres-Lugo, M.; Garcia, M.; Record, R.; Peppas Nicholas, A. *Biotechnol. Prog.* **2002**, *18*, 612−616.
(30) Hourdet, D.; L'Alloret, F.; Audebert, R. *Polymer* **1997**, *38*, 2535−2547.
(31) Ito, K.; Tanaka, K.; Tanaka, H.; Imai, G.; Kawaguchi, S.; Itsuno, S. *Macromolecules* **1991**, *24*, 2348−2354.
(32) Tan, J. S.; Gasper, S. P. *Macromolecules* **1973**, *6*, 741−746.
(33) Silverstein, R. M.; Webster, F. X. *Spectrometric Identification of Organic Compounds*, 6th ed.; 1997.
(34) Uemura, Y.; Macdonald, P. M. *Macromolecules* **1996**, *29*, 63−69.
(35) Luesse, S.; Arnold, K. *Macromolecules* **1996**, *29*, 4251−4257.
(36) Iliopoulos, I.; Halary, J. L.; Audebert, R. *J. Polym. Sci., Part A: Polym. Chem.* **1988**, *26*, 275−284.
(37) Stejskal, E. O.; Tanner, J. E. *J. Chem. Phys.* **1965**, *42*, 288−292.

MA035261I